Supporting Information:

Size-Selective Nanoparticle Assembly on Substrates by DNA Density Patterning

Benjamin D. Myers[1,2], *Qing-Yuan Lin*[1], *Huanxin Wu*[3], *Erik Luijten*[1,3,4], *Chad A. Mirkin*[1,5,6] *and Vinayak P. Dravid**[1,2,5]

1. Department of Materials Science and Engineering, Northwestern University, Evanston, Illinois 60208, United States

2. NU*ANCE* Center, Northwestern University, Evanston, Illinois 60208, United States

3. Department of Physics and Astronomy, Northwestern University, Evanston, Illinois 60208, United States

4. Department of Engineering Sciences and Applied Mathematics, Northwestern University, Evanston, Illinois 60208, United States

5. International Institute for Nanotechnology, Northwestern University, Evanston, Illinois 60208, United States

6. Department of Chemistry, Northwestern University, Evanston, Illinois 60208, United States

* Corresponding Author: v-dravid@northwestern.edu

Spectrophotometry of Nanoparticle Film Melting

Temperature-controlled spectrophotometry was used to study the melting behavior of nanoparticle films. The same nanoparticle assembly procedure described above was used to create uniform nanoparticle films (no electron-beam patterning) on Cr/Au coated quartz substrates. The quartz substrates with nanoparticle films were immersed in storage buffer in quartz cuvettes. A spectrophotometer (Cary 5000) was used to monitor the absorption peak for the gold nanoparticles as the samples were heated from 20 °C to 60 °C at a rate of 0.1 °C/min. The absorption peak for 30 nm nanoparticles was near 534 nm, and near 540 nm for 80 nm nanoparticles. As shown in Figure S1, the melting temperature (50% absolute change in absorbance) was found to be 48.9 °C for 30 nm particles and 53.1 °C for 80 nm particles.

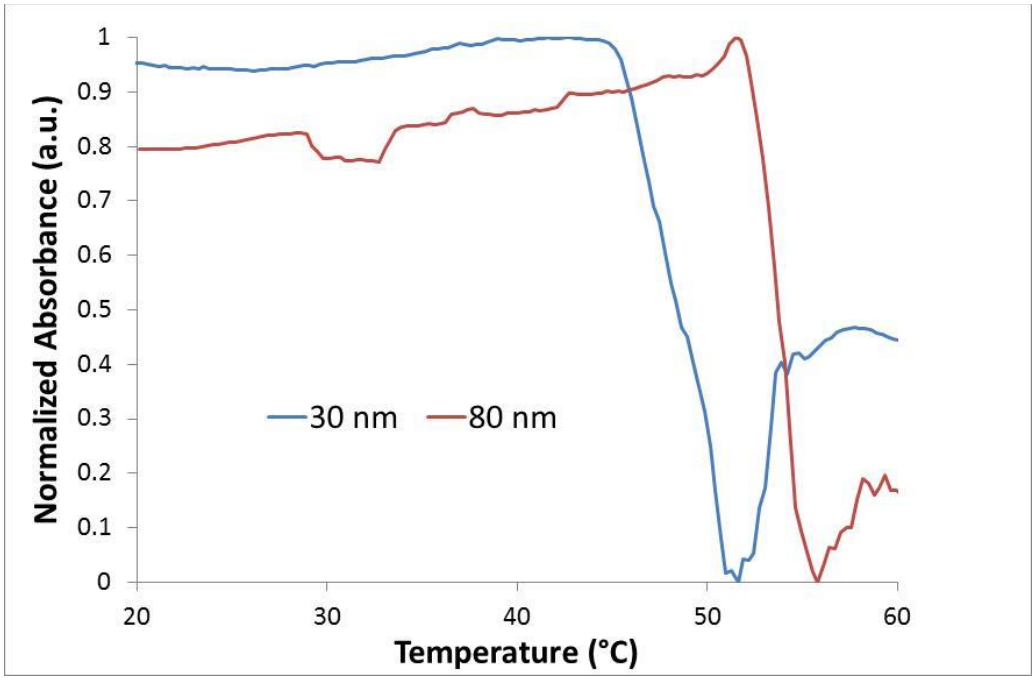

Figure S1. Temperature-dependent UV-vis melting curves for 30 and 80 nm nanoparticle films.

Lower Concentration Ratio Assembly and Effects of Linker Concentration

A series of experiments was conducted to verify that the size-selective assembly process was not dependent on high nanoparticle concentrations or the high ratio of small to larger particles. Separate batches of 30 nm and 80 nm nanoparticles and substrates were functionalized as described in Section S1. These particles were mixed in concentration ratios (30 nm:80 nm) of 5:1 and 10:1 with lower total concentrations of 600 pM and 550 pM, respectively. Similar size-selectivity was noted as in the high-concentration, high-ratio study (Fig. S2). However, the concentration of linker DNA relative to the nanoparticle concentration was found to be critical to observe size-selective assembly. Initial linker concentrations were adapted from the literature,[1] but in the lower-concentration experiments this linker concentration proved insufficient for effective size selection (Fig. S3a). We hypothesize that this is due to insufficient loading of linker oligonucleotides on the nanoparticles. On the other hand, at higher linker concentrations, size-selective assembly was still not observed, likely due to excess linker in solution competing with nanoparticle assembly (Fig. S3b). In fact, the excess linker prevented nearly all adsorption of the 30 nm particles and strongly impacted the adsorption of 80 nm particles in the electron-beam modified regions, even at a significantly lower dose than in other experiments. However, after the nanoparticles were centrifuged and resuspended three times to remove excess linker, strong size-selective assembly was observed (Fig. S3c). This indicates that the particles were densely loaded and supports the notion that free linker strands can compete with nanoparticles and impact adsorption properties.

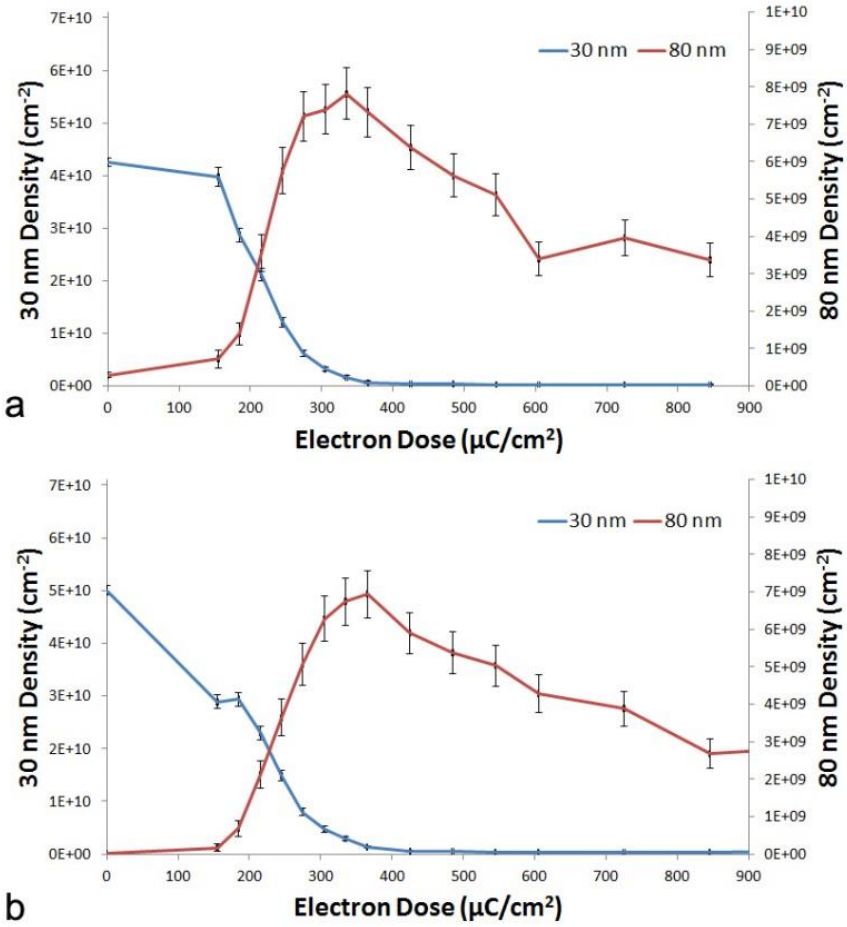

Figure S2. Areal density as a function of electron dose for lower-concentration and lower-ratio size-selective assembly at 35 °C for a) 500 pM 30 nm/100 pM 80 nm and b) 500 pM 30 nm/50 pM 80 nm.

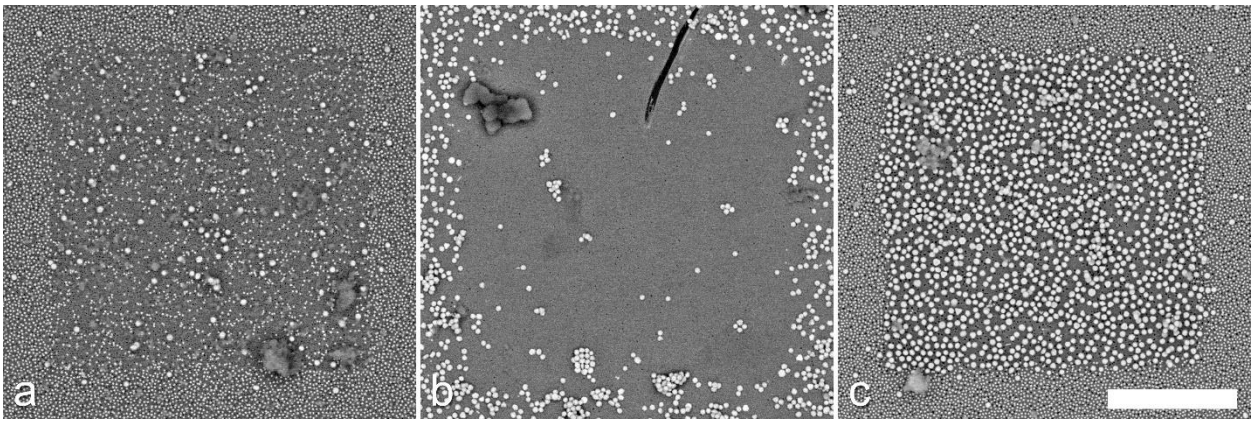

Figure S3. Effects of linker concentration with 500 pM 30 nm/50 pM 80 nm particle solution in 500 μL storage buffer with a) 120 pmol linker DNA and 125 μC/cm^2 electron dose, b) 370 pmol linker DNA and 125 μC/cm^2 electron dose and c) linker DNA removed by centrifugation and resuspension and 425 μC/cm^2 electron dose. All particles were assembled at 35 °C. (Scale bar is 2 μm.)

Image Processing

SEM images were processed with a custom MatLab script to extract the areal densities of both large and small particles as a function of electron dose. The procedure (Fig. S4) involves cropping a region of interest and manually removing polygonal regions from the image which include sol-gel debris, etc. These regions are stored as a mask layer to calculate the total area removed for the areal density calculation. The mask layer is applied to the original image and a threshold operation is applied to create a binary image, which is then processed by a watershed filter to separate particles that may be touching. Due to the polydispersity of the nanoparticles, small particles with diameters of 20–40 nm and large particles with diameters of 65–90 nm were counted and divided by the total analyzed area (excluding the masked regions) to compute the areal density.

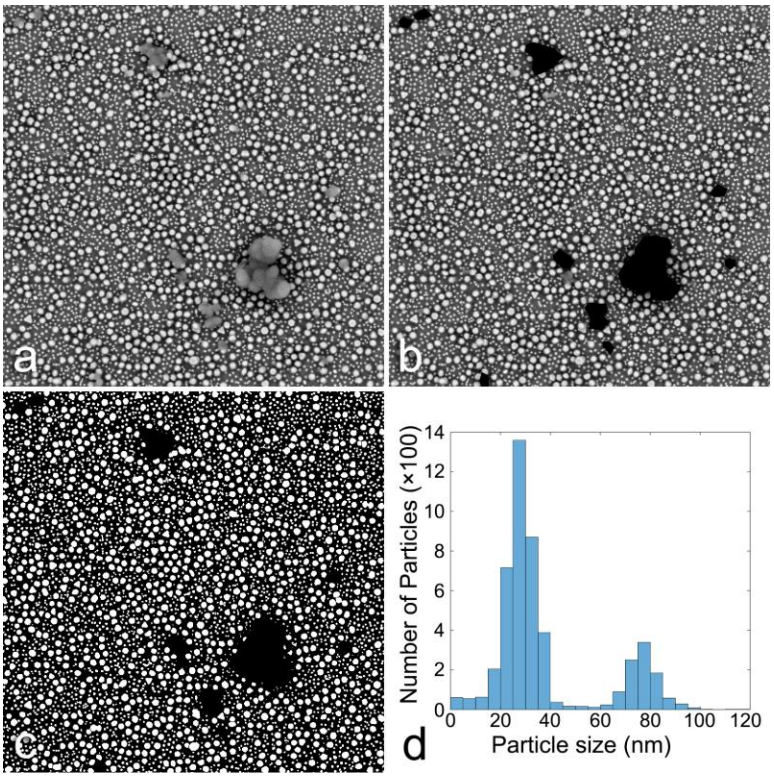

Figure S4. Image processing routine showing a) cropped region of interest, b) regions edited out of analyzed area, c) image threshold and watershed filter applied and d) histogram of particle size.

Particle-Surface Interaction Calculation

The preferential adsorption of smaller particles in regions of high DNA density from a bimodal suspension can be explained by a thermodynamic driving force to maximize the number of hybridized DNA strands. The total enthalpic contribution of the adsorbed particles is directly proportional to the total contact area between the particles and the surface and the density of DNA. Following previous calculations,[2] we compare the ratio of surface interaction area for close-packed particles of different sizes (30 and 80 nm) on a substrate. The DNA-functionalized nanoparticles and substrate are treated as having "fuzzy" surfaces where the sticky ends of the

DNA linkers exist in some predictable range of distances from their respective surfaces. As a result, the degree of binding between particles and surfaces depends on the number of DNA linkages in the region where the two "fuzzy" surfaces interpenetrate as illustrated in Figure S5. Since the substrate DNA density is lower than the particles due to curvature effects,[3] the substrate DNA density will limit the total particle-surface interaction. Therefore, we can ignore the surface area of the particle and simply consider the area of interaction on the substrate when comparing the favorability of adsorption for small and large particles.

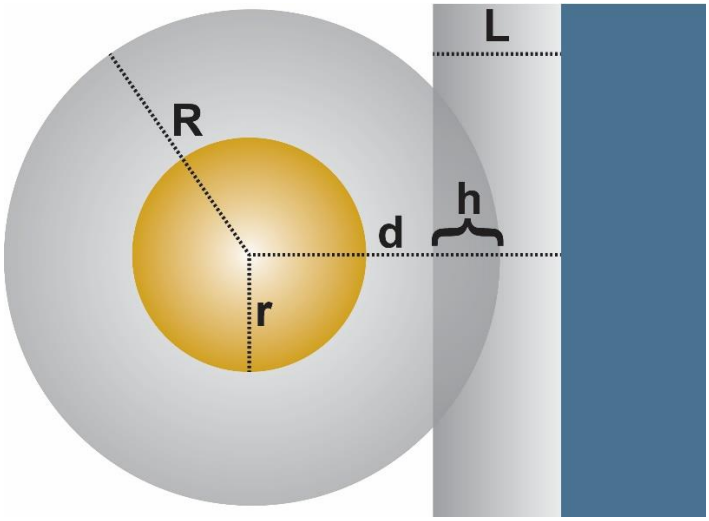

Figure S5. Illustration of geometric interaction between a "fuzzy" nanoparticle and substrate showing relevant variables in calculating the total interaction area for nanoparticle films: *R* is the hydrodynamic radius of the DNA-functionalized nanoparticle, *L* is the fully extended length of the DNA on the substrate, *d* is the nanoparticle-substrate separation when bound by hybridized DNA, *r* is the gold nanoparticle radius and *h* is the overlap of the two "fuzzy" surfaces giving rise to the concept of a contact area.

The particle-to-surface distance (d, in nm) can be calculated by the following:

$$d = r + 0.255x + 0.8\,, \tag{S1}$$

where r is the radius of the inorganic nanoparticle core, x is the total number of nucleobases in the DNA connecting the particles and substrate and 0.8 nm represents the length of two propyl-thiol moieties. The multiplier of 0.255 nm indicates the rise per base pair and has been determined experimentally to represent typical particle separation.[4] To determine the region of overlap between the two "fuzzy" surfaces, the distance d is compared to the hydrodynamic radius (R, in nm) of the "fuzzy" nanoparticle,

$$R = r + 0.34y + 0.4\,, \tag{S2}$$

and the thickness of the DNA layer on the substrate (L, in nm) can be calculated similarly,

$$L = 0.34y + 0.4\,, \tag{S3}$$

where y is the total number of nucleobases attached to the nanoparticle and 0.4 nm represents the length of the propyl-thiol moiety. The multiplier of 0.34 nm indicates the rise per base pair for canonical B-form DNA. While the actual values of the rise per base pair were not measured for our experimental conditions, we believe the values used in Equations 1 and 2 are reasonable estimates. Moreover, even if there is some deviation, the relative comparison between small and large particles is still valid. The overlap of the two "fuzzy" surfaces h can then be calculated as

$$h = L - (d - R) \tag{S4}$$

and the area of intersection on the substrate A follows as

$$A = \pi h(2R - h). \tag{S5}$$

To compare the relative surface coverage for particles of different size, a hexagonally close-packed 2D nanoparticle film is used as a reference. Given this arrangement, the maximum surface coverage can be calculated from the following:

$$\%Coverage = 100\left(\frac{A}{2\sqrt{3}R^2}\right). \tag{S6}$$

The results of this calculation indicate that a nanoparticle film made of entirely small (30 nm) particles will result in approximately 41.3% surface coverage while the large (80 nm) particles provide only 23.0% coverage, resulting in a 1.8-fold larger number of DNA linkages for a small particle film.

Molecular Dynamics Simulation

Molecular dynamics simulations using a coarse-grained model were performed to study the microscopic bonding behavior of DNA-functionalized nanoparticles on the DNA-coated substrate as a function of surface modification level. Each grafted DNA strand was modeled as a bead–spring polymer consisting of 14 beads, each of diameter σ = 2 nm, approximately representing the width of double-stranded DNA (ds-DNA). In accordance with experiment, the diameters and the masses of the gold cores of the small and large colloids were chosen to be 15σ (mass $1100m_0$) and 40σ (mass $27500m_0$), respectively, where m_0 is the mass of a DNA bead. The mass ratio does not exactly correspond to the size ratio, but this is immaterial for static properties. We grafted 20 chains on each small colloid and 40 chains on each large colloid. The chains were evenly distributed on the spherical surfaces, according to a modified spiral algorithm.[5] The coverage on the larger colloids (relative to the smaller colloids) was scaled down compared to experiment to reduce the computing time; nevertheless, this choice provides a qualitative correspondence to the experimental system. Each chain was grafted to the sphere at a single point. The excluded-volume interactions between all particles were modeled with an expanded shifted-truncated Lennard-Jones potential with repulsive strength equal to the thermal energy k_BT,

$$u_{\mathrm{LJ}}(r_{ij}) = \begin{cases} \infty & \text{if } r_{ij} \le \Delta_{ij} \\ 4k_BT\left[\left(\frac{\sigma}{r_{ij}-\Delta_{ij}}\right)^{12} - \left(\frac{\sigma}{r_{ij}-\Delta_{ij}}\right)^{6} + \frac{1}{4}\right] & \text{if } \Delta_{ij} < r_{ij} < \Delta_{ij} + 2^{\frac{1}{6}}\sigma \\ 0 & \text{if } r_{ij} \ge \Delta_{ij} + 2^{\frac{1}{6}}\sigma \end{cases} . \quad \text{(S7)}$$

Here, $\Delta_{ij} = r_i + r_j - \sigma$, where r_i and r_j are the radii of two particles. Additionally, the beads within each grafted DNA chain are bonded via a harmonic potential,

$$u_{\text{bond}} = k(r - r_o)^2 \ , \tag{S8}$$

with $r_o = 0.84\sigma$ and $k = 165\ k_B T/\sigma^2$.[6]

In experiments, the DNA is grafted to the colloid by a thiol linkage and consists of a length of single-stranded DNA (ss-DNA) which acts as a spacer, followed by a length of ds-DNA and ss-DNA "sticky end" for binding to the substrate. To model the stiffness of the ds-DNA portion, a dihedral potential was applied with $\theta_o = \pi$ and $k_\theta = 5\ k_B T$ between beads number 4 through 13 in each grafted chain,

$$u_{\text{angle}} = k_\theta(\theta - \theta_o)^2 \ . \tag{S9}$$

To maintain conditions similar to the experiment, 8 large colloids and 88 small colloids were placed in a rectangular simulation box ($140\times140\times280\sigma^3$) with periodic boundary conditions in the *X* and *Y* directions. At the upper and lower *Z* boundaries, repulsive Lennard-Jones walls were placed. To represent the substrate, a 2D lattice of particles of size σ with lattice spacing 3σ was placed at the lower *Z* boundary and served as potential binding sites. We randomly selected a fraction of the lattice particles to be inactive to represent a certain degree of surface modification by electron beam irradiation. To simulate the DNA hybridization, we employed dynamic bonding functions to form and break bonds between the active surface sites and the tail bead of any grafted DNA. When separated by a distance equal to or less than $2^{1/6}\sigma$, a harmonic bond was formed with $r_o = 2^{1/6}\ \sigma$ and $k = 165\ k_B T/\sigma^2$. Such a bond would break if subsequently the bond length equaled or exceeded 1.4σ with a critical energy of 12.7 $k_B T$. Each active surface site could only bind with one DNA strand at any given time.

Starting from an initial configuration, we gradually increased the time step to 0.015τ, where $\tau = (m_0\sigma^2/k_BT)^{1/2}$ is the reduced time unit. A Langevin thermostat with damping time 10τ was used for temperature control. For each simulation, the grafted DNA chains were first allowed to equilibrate over 84τ, during which the colloids were kept fixed in space. This was followed by a global equilibration period of $4.5\times10^5\tau$. Statistics were then collected for another $4.5\times10^5\tau$ with the surface binding configurations collected every 7.5 τ. For 20 equally spaced modification levels between 0 and 100% we performed 20 independent runs.

References

1. Senesi, A. J.; Eichelsdoerfer, D. J.; Brown, K. A.; Lee, B.; Auyeung, E.; Choi, C. H. J.; Macfarlane, R. J.; Young, K. L.; Mirkin, C. A. Oligonucleotide Flexibility Dictates Crystal Quality in DNA-Programmable Nanoparticle Superlattices. *Adv. Mater.* **2014**, 26, 7235-7240.

2. Macfarlane, R. J.; Lee, B.; Jones, M. R.; Harris, N.; Schatz, G. C.; Mirkin, C. A. Nanoparticle Superlattice Engineering with DNA. *Science* **2011**, 334, 204-208.

3. Hill, H. D.; Millstone, J. E.; Banholzer, M. J.; Mirkin, C. A. The Role Radius of Curvature Plays in Thiolated Oligonucleotide Loading on Gold Nanoparticles. *ACS Nano* **2009**, 3, 418-424.

4. Hill, H. D.; Macfarlane, R. J.; Senesi, A. J.; Lee, B.; Park, S. Y.; Mirkin, C. A. Controlling the Lattice Parameters of Gold Nanoparticle Fcc Crystals with Duplex DNA Linkers. *Nano Lett.* **2008**, 8, 2341-2344.

5. Vogel, H. A Better Way to Construct the Sunflower Head. *Math. Biosci.* **1979**, 44, 179-189.

6. Li, T. I.; Sknepnek, R.; Macfarlane, R. J.; Mirkin, C. A.; Olvera de la Cruz, M. Modeling the Crystallization of Spherical Nucleic Acid Nanoparticle Conjugates with Molecular Dynamics Simulations. *Nano Lett.* **2012**, 12, 2509-2514.